Lessons from Hurricane Katrina Storm Surge on Bridges and Buildings

Article *in* Journal of Waterway Port Coastal and Ocean Engineering · November 2007

DOI: 10.1061/(ASCE)0733-950X(2007)133:6(463)

4 authors:

Ian Nicol Robertson
University of Hawai'i at Mānoa
101 PUBLICATIONS **484** CITATIONS
SEE PROFILE

H.R. Riggs
University of Hawai'i at Mānoa
128 PUBLICATIONS **1,030** CITATIONS
SEE PROFILE

Solomon C Yim
Oregon State University
162 PUBLICATIONS **1,226** CITATIONS
SEE PROFILE

Yin Lu Young
University of Michigan
131 PUBLICATIONS **1,287** CITATIONS
SEE PROFILE

Lessons from Hurricane Katrina Storm Surge on Bridges and Buildings

Ian N. Robertson[1]; H. Ronald Riggs[2]; Solomon C. S. Yim[3]; and Yin Lu Young[4]

Abstract: The storm surge associated with Hurricane Katrina caused tremendous damage along the Gulf Coast in Louisiana, Mississippi, and Alabama. Similar damage was observed subsequent to the Indian Ocean tsunami of December 26, 2004. In order to gain a better understanding of the performance of engineered structures subjected to coastal inundation due to tsunami or hurricane storm surge, the writers surveyed damage to bridges, buildings, and other coastal infrastructure subsequent to Hurricane Katrina. Numerous lessons were learned from analysis of the observed damage, and these are reported herein. A number of structures experienced significant structural damage due to storm surge and wave action. Structural members submerged during the inundation were subjected to significant hydrostatic uplift forces due to buoyancy, enhanced by trapped air pockets, and to hydrodynamic uplift forces due to wave action. Any floating or mobile object in the nearshore/onshore areas can become floating debris, affecting structures in two ways: impact and water damming. Foundation soils and foundation systems are at risk from shear- and liquefaction-induced scour, unless designed appropriately.

DOI: 10.1061/(ASCE)0733-950X(2007)133:6(463)

CE Database subject headings: Storm surge; Hurricanes; Tsunamis; Coastal structures; Hydraulic loads; Debris; Structural failures.

Introduction

General

Hurricane Katrina is likely to be the most expensive natural disaster in U.S. history. It developed as a category 5 storm in the Gulf of Mexico before making landfall on the border between Louisiana and Mississippi as a category 3 storm (FEMA 2006a,b). As expected from a storm of this magnitude, there was considerable wind and rain damage. However, the primary cause of damage to coastal infrastructure along the entire Mississippi coastline, and portions of the Louisiana and Alabama coastlines, was the inundation due to storm surge and wind-induced wave action. This damage far exceeded the wind-induced and storm surge damage caused by any prior hurricane or tsunami impacting the U.S. coastline. Similar damage was observed along coastlines affected by the Indian Ocean tsunami of December 26, 2004 (CAEE 2005).

This paper presents some of the lessons learned from our investigation of the performance of engineered structures, including reinforced and prestressed concrete buildings, coastal bridges, and barge-mounted casinos, when subjected to Hurricane Katrina storm surge. Our investigation did not include the effects of flooding in New Orleans since this was a result of levee failure, and not directly due to storm surge and wave action on the affected buildings. Similar postdisaster assessments are common after hurricane and tsunami events (FEMA 2006a; Dengler and Magoon 2005; Rogers 2005; Tezak and Rogers 2005; Saatcioglu et al. 2005); however, the primary focus has normally been the performance of wood-framed residential structures. Subsequent to Hurricane Katrina, some assessment teams have included the response of engineered structures in their postevent surveys (FEMA 2006b; Mosqueda and Porter 2006; Douglass et al. 2006).

Storm Surge

The peak storm surge caused by Hurricane Katrina exceeded 7.5 m (25 ft) above sea level and occurred between Pass Christian and Gulfport, confirming computer model predictions made by the Louisiana Hurricane Research Center just days before landfall (LSU 2005). This level of surge is considerably greater than that experienced during other recent hurricanes of similar intensity, primarily because of the shallow coastal bathymetry and the shape of the coastline and man-made levees around the Mississippi River delta (FEMA 2006b). In addition, the storm surge and wind-induced wave action would have developed while Katrina was a Category 5 hurricane in the Gulf of Mexico. Although wind speeds had declined to Category 4 as Katrina made landfall on the Mississippi River delta, and Category 3 at the Louisiana/Mississippi border, the storm surge and wave action may not have abated as rapidly.

Of particular interest to the writers, and the primary reason for their reconnaissance trips to the Mississippi coastline, was the effect of the storm surge on engineered structures. The extent of storm surge damage to engineered infrastructure along the Gulf Coast was greater than might have been anticipated. Numerous lessons can be learned from this event to aid in design and

[1]Professor, Dept. of Civil and Environmental Engineering, Univ. of Hawaii at Manoa, Honolulu, HI.

[2]Professor and Chairman, Dept. of Civil and Environmental Engineering, Univ. of Hawaii at Manoa, Honolulu, HI.

[3]Professor, Dept. of Civil, Construction and Environmental Engineering, Oregon State Univ., Corvallis, OR.

[4]Assistant Professor, Dept. of Civil and Environmental Engineering, Princeton Univ., Princeton, N.J.

Note. Discussion open until April 1, 2008. Separate discussions must be submitted for individual papers. To extend the closing date by one month, a written request must be filed with the ASCE Managing Editor. The manuscript for this paper was submitted for review and possible publication on June 14, 2006; approved on January 25, 2007. This paper is part of the ***Journal of Waterway, Port, Coastal, and Ocean Engineering***, Vol. 133, No. 6, November 1, 2007. ©ASCE, ISSN 0733-950X/2007/6-463–483/$25.00.

Fig. 1. Reinforced concrete single-family residence owner-designed by a structural engineer

construction of future bridges and buildings, and retrofit of existing structures, in regions subject to storm surge or tsunami inundation.

Damage to Residential Construction

The effect of the storm surge coastal inundation was particularly devastating for light-framed wood and unreinforced masonry residential structures. In many coastal communities the only remaining evidence of residential construction was the ground-floor slab on grade and considerable piles of debris at the high water mark. There were some notable exceptions where residential buildings were able to survive substantial surge inundation. These exceptions were often constructed with concrete or steel frames, and elevated above grade. One of these buildings was a single-family residence, designed and owned by a structural engineer (Fig. 1). It was able to withstand inundation and wave action to the mid-height of the second level without suffering any structural damage. Many of the lessons relating to residential construction are included in a FEMA Mitigation Assessment Team (MAT) report published shortly after this event (FEMA 2006b).

Damage to Engineered Structures

The focus of this paper is the effect of coastal inundation on engineered structures. The primary factors causing damage to engineered structures were hydrostatic uplift, hydrodynamic uplift and lateral loading, restraint failure, debris effects, and scour. Each of these factors is considered in detail in the sections that follow, resulting in a number of conclusions that can be applied to future coastal construction and retrofit of existing buildings and bridges.

Structural Loading

Bea et al. (1999) define the total force acting on decks of offshore platforms due to wave action as a combination of force vectors

$$\mathbf{F_{tw}} = \mathbf{F_b} + \mathbf{F_s} + \mathbf{F_d} + \mathbf{F_l} + \mathbf{F_i} \tag{1}$$

where $\mathbf{F_b}$=vertical buoyancy force; $\mathbf{F_s}$=horizontal slamming force; $\mathbf{F_d}$=horizontal hydrodynamic drag force; $\mathbf{F_l}$=vertical hydrodynamic uplift force; and $\mathbf{F_i}$=acceleration-dependent inertia force. Based on an analysis of the performance of bridge decks during Hurricane Katrina, Douglass et al. (2006) conclude that the horizontal hydrodynamic force, $\mathbf{F_d}$, and the vertical hydrodynamic uplift force, $\mathbf{F_l}$, were the primary loads inducing failure. However, since many bridge decks and elevated floors in buildings were completely submerged during the hurricane, vertical buoyancy forces, $\mathbf{F_b}$, also must be considered. In the analysis that follows, these symbols are shown without bold to indicate the vector magnitude.

Horizontal Hydrodynamic Load

Douglass et al. (2006) propose the following expression for the horizontal hydrodynamic load, F_d, induced by wave action on bridge decks:

$$F_d = [1 + c_r(N-1)]c_{h-va}\gamma(\Delta z_h)A_h \tag{2}$$

where c_r=reduction coefficient for horizontal load on all bridge girders except the wave-ward girder, with a recommended value of 0.4; N=number of girders supporting the bridge deck; c_{h-va}=empirical coefficient with a recommended value of 1.0; γ=unit weight of water taken as 10.06 kN/m^3 (64 lb/ft^3) for seawater; Δz_h=difference between the elevation of the crest of the

Table 1. Horizontal Hydrodynamic Load Calculations for Bridges Investigated in This Study

Bridge	Assumed surge level	Assumed maximum wave height above surge level m (ft)	Elevation of centroid of deck edge above surge level m (ft)	Vertical projection of edge of bridge deck m (ft)	Number of girders	Horizontal hydrodynamic load per unit length of bridge deck kN/m (lb/ft)	Horizontal hydrodynamic load on single span of bridge deck kN (lb)
US 90–Biloxi Bay	3.63 m (11.9 ft[a]) (1.1 ft below bottom of bridge girders)	2.46 (8.06[a])	1.16 (3.8[a])	1.68 (5.5[a])	6	65.9[b] (4,500[a])	1,041 (234,000[a])
Old bridge–Biloxi Bay	At bottom of bridge girders	2.46 (8.06[a])	0.55 (1.79)	1.09 (3.58)	3	37.7 (2,585)	414 (93,000)
Railroad bridge–Biloxi Bay	At bottom of bridge girders	2.46 (8.06[a])	1.05 (3.46)	2.11 (6.92)	4[c]	47.9 (3,260)	891 (198,860)
US 90–Bay St. Louis[d]	At bottom of bridge girders	2.5[d](8.2)	0.65 (2.13)	1.30 (4.25)	4	53.2 (3,632)	665 (148,900)
Railroad bridge–Bay St. Louis[d]	At bottom of bridge girders	2.5[d](8.2)	0.93 (3.04)	1.85 (6.08)	1 (box)	29.2 (2,008)	543 (122,500)
US 90 approach span–Pass Christian[e]	Unknown	Unknown	—	2.97 (9.75)	6	—	—
I-10 Onramp–Mobile	At bottom of bridge girders	2.22 (7.28[a])	0.96 (3.15)	1.92 (6.29)	4	53.5 (3,658)	816 (182,900)

[a]Douglass et al. (2006).

[b]Sample calculation using Eq. (2): $[1+0.4(6-1)]^{*}1^{*}10.06(2.46-1.16)^{*}1.68=65.9$ kN/m.

[c]Girders very closely spaced—assumed $c_r=0.2$.

[d]Assumed wave heights.

[e]Surge level and wave heights unknown.

maximum wave and the elevation of the centroid of A_h; and A_h=area of projection of the bridge deck onto a vertical plane.

By coupling the ADCIRC (advanced circulation) surge model and the SWAN (simulation of waves in nearshore areas) wave model, Chen et al. (2005) provide surge and wave height estimates for Biloxi Bay during Hurricane Katrina. Douglass et al. (2006) utilized these estimates to determine the hydrodynamic lateral load on a typical 15.8 m (52 ft) long deck segment of the US 90 highway bridge over Biloxi Bay, Mississippi, at 1,041 kN (234,000 lb) (Douglass et al. 2006). This represents a distributed lateral load of 65.9 kN/m (4,500 lb/ft) along the length of the bridge deck. The wave heights and bridge dimensions used by Douglass et al. (2006) in computing this load are listed in the second row of Table 1.

In addition to the US 90 highway bridge over Biloxi Bay, the writers investigated six other coastal bridges during this study. The old highway bridge and railroad bridge over Biloxi Bay are located adjacent to the US 90 highway bridge and are assumed to have been subjected to the same wave heights. The relevant bridge dimensions and resulting horizontal hydrodynamic loads from Eq. (2) are listed in the third and fourth rows of Table 1. Two bridges over Bay St. Louis suffered loss of virtually all low-level bridge deck segments, namely the US 90 highway bridge and a box-girder railroad bridge. Although wave height modeling is not available for Bay St. Louis, wave heights were assumed similar to those predicted for Biloxi Bay, based on their proximity to the maximum storm surge that occurred between the two bays. The fifth and sixth rows of Table 1 list the assumed wave and surge heights, along with relevant bridge dimensions and resulting horizontal hydrodynamic load from Eq. (2) for these bridges.

The US 90 approach span in Pass Christian is some distance inland from the shoreline. Since no surge level or wave height estimates are available for this bridge, the hydrodynamic loads were not computed. Finally, the I-10 on-ramp in Mobile, Alabama, experienced lateral movement of five low-level deck segments, though none fell off the supporting piers. Douglass et al. (2006) estimated the wave heights at this bridge at 2.22 m (7.28 ft). This estimate, along with relevant bridge dimensions and the resulting horizontal hydrodynamic load, are listed in the eighth row of Table 1.

The hydrodynamic lateral loads in Table 1 are compared with the lateral restraint provided by the support bearings and shear keys later in this paper.

Hydrodynamic Uplift

Based on a review of current literature and experimental results, Douglass et al. (2006) propose the following expression for the vertical hydrodynamic uplift load, F_l, produced by wave action on bridge decks:

$$F_l = c_{v-va}\gamma(\Delta z_v)A_v \tag{3}$$

where c_{v-va}=empirical coefficient with a recommended value of 1.0; Δz_v=difference between the elevation of the crest of the maximum wave and the elevation of the underside of the bridge deck; and A_v=area of the projection of the bridge deck onto a horizontal plane.

Douglass et al. (2006) utilize the previous estimates of surge level and wave height to determine the hydrodynamic uplift on a typical deck segment of the US 90 bridge over Biloxi Bay, Mississippi, at 1,957 kN (440,000 lb). This represents an uplift of 123.6 kN/m (8,465 lb/ft) along the length of the bridge deck, as shown in the second row of Table 2. Based on the assumed surge levels and wave heights described earlier for the other six bridges investigated during this study, estimates of the hydrodynamic uplift from Eq. (3) are provided in Table 2.

The estimated hydrodynamic uplift exceeds the self-weight of the bridge deck by over 30% for all bridges except the railroad bridges over Biloxi Bay and Bay St. Louis. The railroad bridge over Biloxi Bay has a self-weight 64% greater than the estimated hydrodynamic uplift, and suffered no span failures during the hurricane. The box-girder railroad bridge over Bay St. Louis has an estimated self-weight of 71.81 kN/m (4,920 lb/ft) based on assumed box wall thicknesses of 30 cm (12 in.). This is only

Table 2. Hydrodynamic Uplift Calculations for Bridges Investigated in This Study

Bridge	Assumed surge level	Assumed maximum wave height above surge level m (ft)	Elevation of bottom of deck above surge level m (ft)	Bridge deck width m (ft)	Hydrodynamic uplift per unit length of bridge deck kN/m (lb/ft)	Self-weight of bridge deck per unit length kN/m (lb/ft)
US 90–Biloxi Bay	3.63 m (11.9 ft[a]) (1.1 ft below bottom of bridge girders)	2.46 (8.06[a])	1.25 (4.1[a])	10.16 (33.4[a])	123.6[b] (8,465[a])	92.76 (6,360[a])
Old bridge–Biloxi Bay	At bottom of bridge girders	2.46 (8.06[a])	0.915 (3.0)	6.94 (22.75)	107.8 (7,367)	56.98 (3,915)
Railroad bridge–Biloxi Bay	At bottom of bridge girders	2.46 (8.06[a])	1.47 (4.83)	5.18 (17.0)	51.6 (3,536)	84.76 (5,820)
US 90–Bay St. Louis[c]	At bottom of bridge girders	2.5[c] (8.2)	0.89 (2.92)	9.58 (31.4)	155.1 (10,611)	92.06 (6,315)
Railroad bridge–Bay St. Louis[c]	At bottom of box girder	2.5[c] (8.2)	1.30 (4.25)	5.34 (17.5)	64.4 (4,424)	71.81 (4,920)
US 90 approach span–Pass Christian[d]	Unknown	Unknown	—	14.74 (48.33)	—	177.8 (12,195)
I-10 Onramp–Mobile	At bottom of bridge girders	2.22 (7.28[a])	0.915 (3.0)	8.64 (28.33)	113.4 (7,760)	69.93 (4,800)

[a]Douglass et al. (2006).

[b]Sample calculation using Eq. (3): $1^{*}10.06(2.46-1.25)(1^{*}10.16)=123.6$ kN/m.

[c]Assumed wave heights.

[d]Surge level and wave heights unknown.

11.5% greater than the estimated hydrodynamic uplift. Most of the spans of this bridge were displaced from the supporting piers during the hurricane. Only six spans remained in place at the Pass Christian end of the bridge, possibly due to reduced wave heights because of a nearby breakwater.

This expression for hydrodynamic uplift is limited to conditions where the still-water level (or surge level) is at or below the bottom of the bridge girders. Once the surge level exceeds the bottom of the girders, the above expression is no longer considered valid, and no guidance is available from current literature for this condition (Douglass et al. 2006). When a bridge deck or similar horizontal structural element becomes partially or fully submerged, the effects of buoyancy, or hydrostatic uplift, become important.

Hydrostatic Uplift

Hydrostatic uplift is defined here as a combination of buoyancy due to submersion in water [F_b in Eq. (1)] and the effect of air trapped below a structural element. Although the water state during a hurricane or tsunami is clearly not static, the hydrostatic uplift is considered separately from the hydrodynamic uplift described in the previous section. Together the hydrostatic and hydrodynamic components make up the total uplift on the structural element.

For hurricane storm surge conditions, the relative importance of hydrodynamic and hydrostatic uplift will depend on the wind-induced wave height at the structure being considered. For tsunami inundation, wave action on top of the tsunami surge is

Fig. 2. Grand Casino, Biloxi, with inland parking garage that suffered collapse of the second-level double-tee floor system (Fig. 11) (Photo courtesy of U.S. National Oceanic and Atmospheric Administration/Department of Commerce)

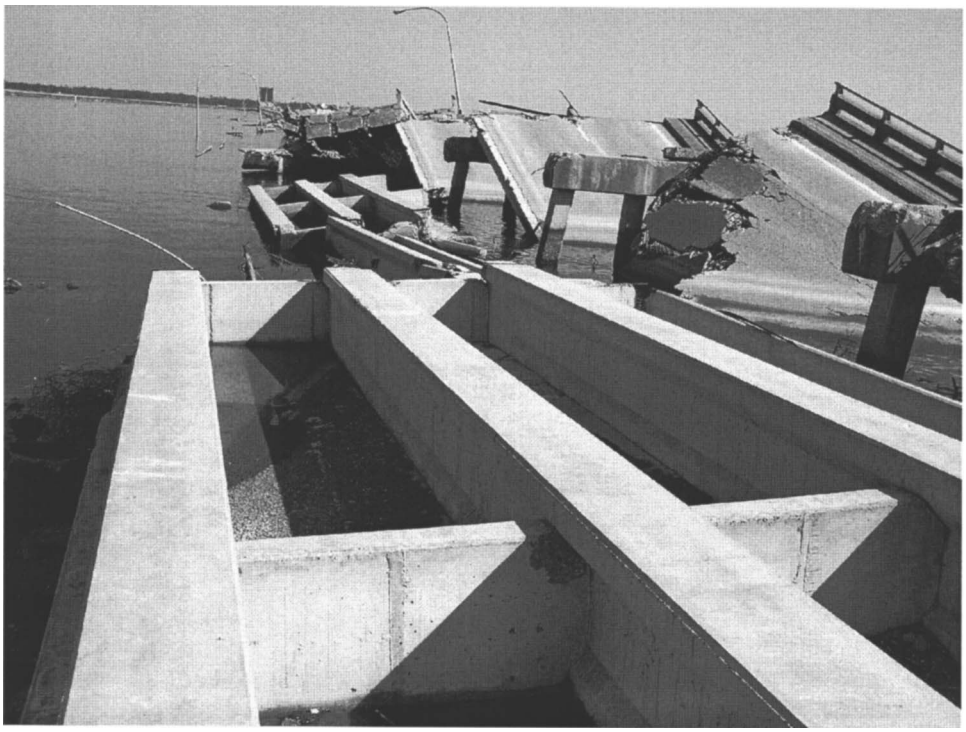

Fig. 3. Girders, bridging, and bulkheads potentially trap air below deck of US 90 highway bridge over Biloxi Bay

substantially less than in the case of hurricane storm surge inundation. In these conditions the buoyancy effect is likely to be more important than the hydrodynamic uplift. It is therefore important to investigate both vertical loading conditions to determine the worst case for a particular structural element.

Numerous low-level coastal bridges were completely submerged by the storm surge. The resulting reduction in self-weight of the bridge spans, combined with buoyancy due to trapped air, would lead to significant hydrostatic uplift. A large number of double-tee slab systems used in parking garages also failed due to excessive uplift. A number of these structures were some distance from the shoreline and protected from wave action by intervening buildings. For example, the inland parking structure at the Grand Casino, Biloxi, is shielded by structures along the shoreline (Fig. 2). In these cases, hydrostatic uplift due to buoyancy is likely the major factor causing failure of the slab system.

Submersion in seawater reduces the effective self-weight of concrete members from around 23.54 kN/m^3 (150 lb/ft^3) to 13.49 kN/m^3 (86 lb/ft^3). In addition, air trapped below the bridge deck or slab system—between the girders, transverse bridging, and end bulkheads—could even provide enough flotation to make the bridge span or double-tee floor system buoyant.

The US 90 highway bridge over Biloxi Bay is composed of simply supported bridge segments varying in length from 13.7 to 15.9 m (45 to 52 ft), each consisting of six prestressed concrete girders supporting half of the roadway deck and one sidewalk. The air trapped between the girders, along with the reduction in self-weight due to submersion in seawater, meant

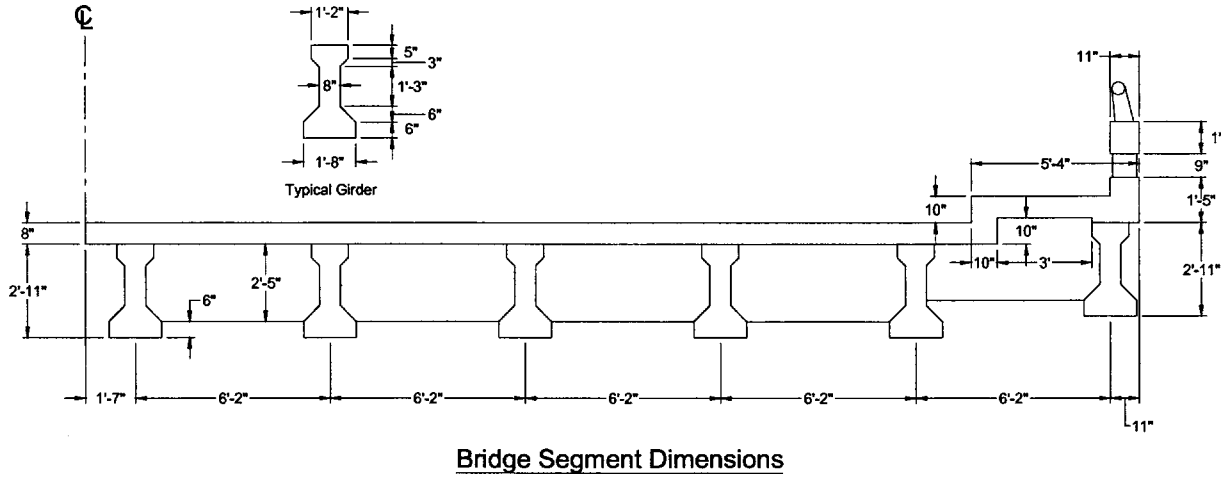

Fig. 4. Cross-section details of US 90 highway bridge over Biloxi Bay (1 ft=0.3048 m)

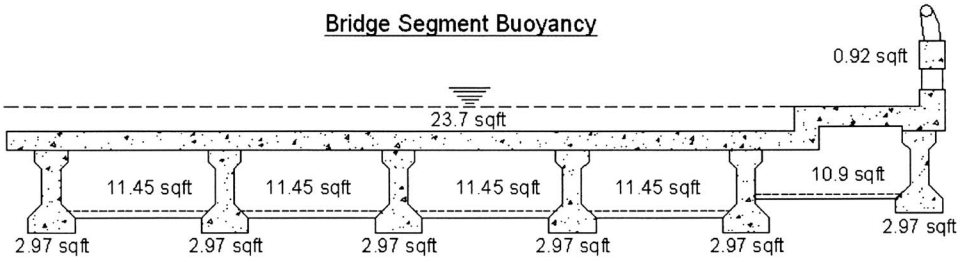

Fig. 5. Buoyancy calculation for US 90 highway bridge over Biloxi Bay (1 ft=0.3048 m, 1 lb=4.445 N)

that these segments were very nearly buoyant once submerged (Fig. 3). Fig. 4 shows the dimensions of a typical cross section of the bridge deck as measured on site, and Fig. 5 outlines the buoyancy calculation performed on this cross section, including the effects of air compressibility.

In the buoyancy calculations, air is assumed to fill the void under the bridge deck when the water level reaches the bottom of the end bulkheads. This volume of air is assumed trapped as the water level rises to submerge the entire deck section. Considering hydrostatic effects only, the water head acting on the trapped air will result in a decrease in the air volume. Assuming constant temperature, the ideal gas law relates pressure, P, and volume, V, at two states

$$P_1V_1 = P_2V_2 \tag{4}$$

where P_1=101.325 kPa (14.7 psi) is the atmospheric pressure at sea level; V_1=original trapped air volume, per unit length along the bridge cross section; P_2=101.325+$h\times$1,025 $\times$9.81/1,000 kPa (=14.7+$h\times$64/144 psi) is the pressure when fully submerged; h=depth of water from the top of sidewalk to the bottom of the compressed air pocket; and V_2=resulting compressed volume of air trapped below the bridge deck used to compute buoyancy effects on the deck section.

The buoyancy analysis results based on in Fig. 5 for the US 90 highway bridge across Biloxi Bay are summarized in Table 3 along with those for six other bridge cross-sections measured during the reconnaissance trips. These calculations are based on a unit length of the bridge cross section. The bridge deck self-weight is also listed in Table 3 as a weight per unit length of the bridge cross section, based on field measurements of each bridge. These self-weights do not include the weight of bulkheads, bridging and other elements making up an entire deck section.

Comparison of the buoyancy and self-weight of each bridge in Table 3 shows that the US 90 approach span in Pass Christian would be fully buoyant if completely submerged, while the US 90 bridge over Biloxi Bay is very close to buoyant when submerged. The only bridge not damaged by the storm surge was the railroad bridge over Biloxi Bay, with a residual dead weight of 39.5% of the unsubmerged self-weight. All other bridges have less than 28% residual self-weight when submerged.

Structural System Response

Bridge Structures

For the US 90 highway bridge across Biloxi Bay, the bearings supporting each end of the girders at the pier bents provided no restraint against uplift and only nominal resistance against lateral movement (Fig. 6). Being a low seismic zone, the region had no requirements for shear keys to provide lateral restraint or ties to prevent uplift, as is common in seismic regions. Friction induced by gravity load, and small 11 mm (7/16 in.) thick steel angles, were the only physical restraint against lateral movement for these bridge segments. When subjected to the wave-induced hydrodynamic uplift (Table 2) and/or buoyancy effects (Table 3), the segments were free to move off their supports under the lateral load from surge and wave action (Table 1). Apart from the bridge segments elevated over the ship channel, every segment of this bridge was dislocated from its supports and collapsed into the bay.

Table 3. Buoyancy Calculations for Bridges Investigated in This Study

Bridge	Concrete volume m^3/m (ft^3/ft)	Air volume m^3/m (ft^3/ft)	Buoyancy[a] force kN/m (lb/ft)	Self-weight[b] kN/m (lb/ft)	Net self-weight kN/m (lb/ft)	Percent of self-weight (%)
US 90—Biloxi Bay[c]	3.94 (42.4)	5.27 (56.7)	91.55 (6,277)	92.76 (6,360)	1.21 (83)	1.3
Old bridge–Biloxi Bay[c]	2.42 (26.1)	2.22 (23.9)	45.46 (3,115)	56.98 (3,915)	11.52 (800)	20.2
Railroad bridge–Biloxi Bay	3.60 (38.8)	1.50 (16.1)	51.28 (3,514)	84.76 (5,820)	33.48 (2,306)	39.5
US 90–Bay St. Louis[c]	3.91 (42.1)	3.21 (34.5)	70.57 (4,836)	92.06 (6,315)	21.49 (1,479)	23.3
Railroad bridge–Bay St. Louis[d]	3.05 (32.8)	2.46 (26.5)	55.37 (3,794)	71.81 (4,920)	16.44 (1,126)	22.9
US 90 approach span–Pass Christian[c]	7.55 (81.3)	17.5 (188.2)	248.4 (17,019)	177.8 (12,195)	−70.6 (−4,824)	−39.7
I-10 Onramp–Mobile[c]	2.97 (32.0)	2.44 (26.28)	50.46 (3,458)	69.93 (4,800)	19.47 (1,342)	27.8

[a]Buoyancy based on 1,025 kg/m^3 (64 lb/ft^3) density of seawater.

[b]Self-weight based on 2,400 kg/m^3 (150 lb/ft^3) density for reinforced concrete.

[c]Assuming guardrails are not submerged.

[d]Assuming box girder stems and base slab are 12 in. thick.

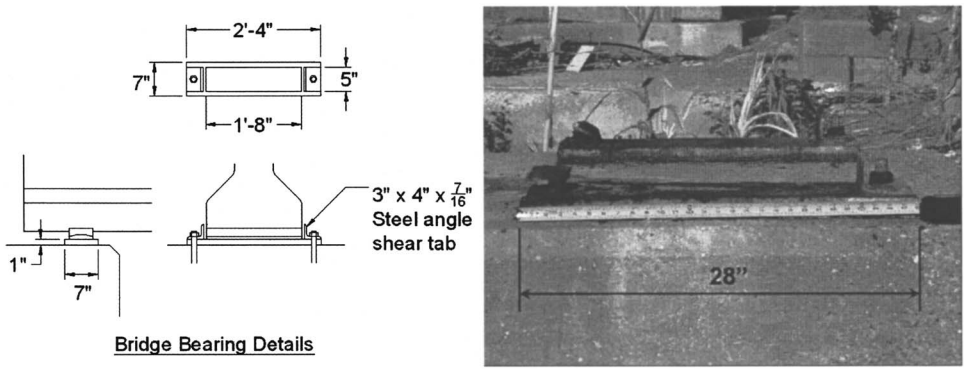

Fig. 6. Bearing restraint details for US 90 highway bridge over Biloxi Bay (1 in.=25.4 mm)

Similar damage occurred at numerous other coastal bridges from the Lake Pontchartrain Causeway and I-10 East of New Orleans to a low-level I-10 on-ramp in Mobile, Alabama. In addition to wave-induced uplift, many of these bridge decks had greatly reduced dead weight due to entrapped air and buoyancy effects.

Even bridges with significant residual self-weight when submerged suffered failures due to inadequate shear keys to prevent lateral movement of the bridge deck segments. For example, the US 90 highway bridge across Bay St. Louis had a residual dead weight of 23.3% when fully submerged (Table 3). The bulkhead and bridging elements provided between the girders of this deck are only partial depth (Fig. 7), allowing much of the air below the deck to escape. Nevertheless, virtually every segment of this bridge was dislodged from the supporting piers. These failures are attributed to the additional effects of hydrodynamic uplift (Table 2) and lateral loads from surge and wave action (Table 1), combined with the lack of restraint against uplift or lateral movement at the support bearings. Fig. 8 shows the rocker bearing at one end of each span. The only restraint against lateral movement of the girders was the three small shear studs provided between the rocker and the bearing plate in the girder soffit.

A notable exception to the poor performance of low-level bridge structures was the railroad bridge over Biloxi Bay. Although the entire railway's tracks, sleepers, and ballast were swept into the bay, the prestressed concrete bridge girders and deck remained intact. The superior performance of this structure is attributed to the reduced hydrodynamic uplift due to the small width of the bridge deck and the relatively small volume of entrapped air because of the closely spaced girders. The wave-induced hydrodynamic uplift is estimated at 51.6 kN/m (3,536 lb/ft) (Table 2), while the hydrostatic uplift (buoyancy) on the submerged deck is estimated at 51.28 kN/m (3,514 lb/ft) (Table 3). Neither of these effects is sufficient to overcome the deck self-weight of 84.76 kN/m (5,820 lb/ft). The maximum uplift due to hydrodynamic and hydrostatic effects will not occur simultaneously since they correspond to different levels of inundation. When the surge level is at the bottom of the girders, the hydrodynamic uplift will be a maximum, but there will be no buoyancy effect. When the surge level is above the top of the roadway, the buoyancy effect will be a maximum, but the hydrodynamic uplift due to wave action will be significantly reduced. To the best of the writers' knowledge, no research has been performed on this condition.

In addition, the superior lateral restraint provided by 380 mm (15 in.) high concrete shear keys on either side of the girders at each support pier (Figs. 9 and 10), was sufficient to resist the lateral hydrodynamic loads (Table 1). Not a single segment of this bridge collapsed.

Double-Tee Floor Systems

As many as 10 different precast parking garages in the Biloxi-Gulfport region suffered major damage or even total collapse of the second-floor level due to the storm surge. Some of these structures were located along the shoreline and were therefore subjected to wave-induced hydrodynamic uplift as well as buoyancy, while others were some distance from the shoreline and protected from wave action by intervening buildings. Fig. 11 shows a typical double-tee floor system collapse in a parking garage that was not directly exposed to wave action (Fig. 2). In these cases, the collapse is attributed entirely to the effects of buoyancy.

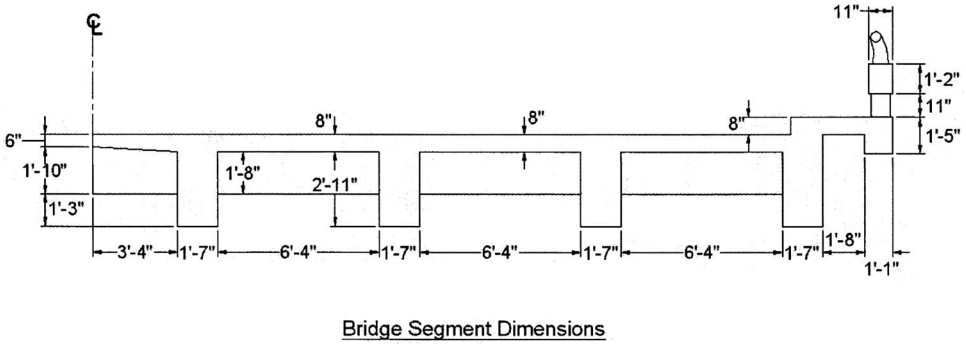

Fig. 7. Cross-section details of US 90 highway bridge over Bay St. Louis (1 ft=0.3048 m, 1 in.=25.4 mm)

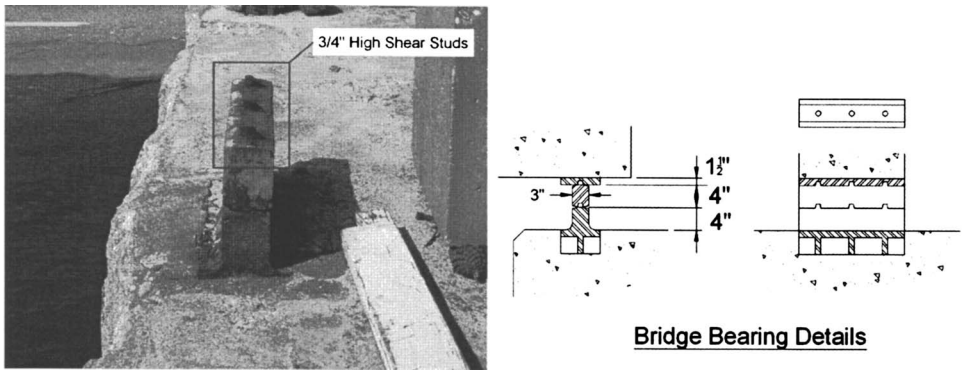

Fig. 8. Rocker bearing details at US 90 highway bridge over Bay St. Louis (1 in.=25.4 mm)

The elevated floors of these precast parking structures consist of prestressed concrete double-tee girders supporting a 50 to 75 mm (2 to 3 in.) thick cast-in-place concrete topping slab. Significant uplift resulted from buoyancy of air trapped between the girder webs below the floor deck (Fig. 12). This air could not escape because of the supporting inverted T-beams or spandrel beams at either end of the span. In addition, the cast-in-place topping slab covers the joint between adjacent double-tees and any gap between the double-tee and the supporting elements at either end of the span. Unable to escape, the air below the floor slab induced uplift well in excess of the submerged dead weight of the double-tee plus topping, resulting in significant negative bending (hogging) of the precast sections.

Table 4 shows buoyancy calculations for various common double-tee sections when submerged in seawater to the top-of-slab elevation. A constant temperature adjustment is made to the entrapped air volume to account for compressibility of the air. Even for the smallest double-tee section observed in any of the inspected garages, with the larger topping thickness of 75 mm (3 in.), the net uplift due to buoyancy exceeds 50% of the original dead weight in air. In other words, the buoyancy due to submersion in seawater and the effect of entrapped air results in a total hydrostatic uplift of 153% of the original dead weight of the section. For deeper and wider sections with thinner topping, this uplift increases to as much as 191%. The situation would be even worse if any of the double-tees and/or topping slabs were constructed of lightweight concrete.

Since the double-tees are designed for gravity load over a simply supported span, they are extremely weak in negative bending. There is typically a light mesh reinforcing in the top flange and topping slab, which are now the tension zone, while the base of the webs is very thin, and the webs now become the compression zone. In addition, the prestressing tendons are located so as to produce uplift intended to balance much of the original unsubmerged dead weight. The combination of uplift due to hydrostatic and prestress effects was sufficient to cause severe cracking of the

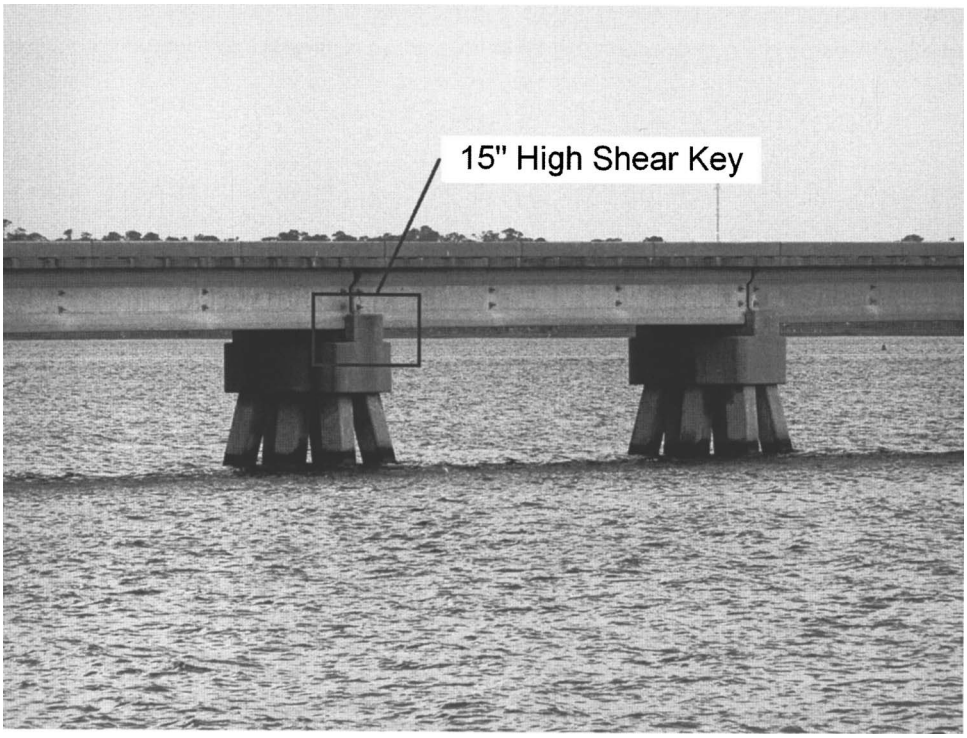

Fig. 9. Railroad bridge over Biloxi Bay with close-spaced girders and large concrete shear keys (1 in.=25.4 mm)

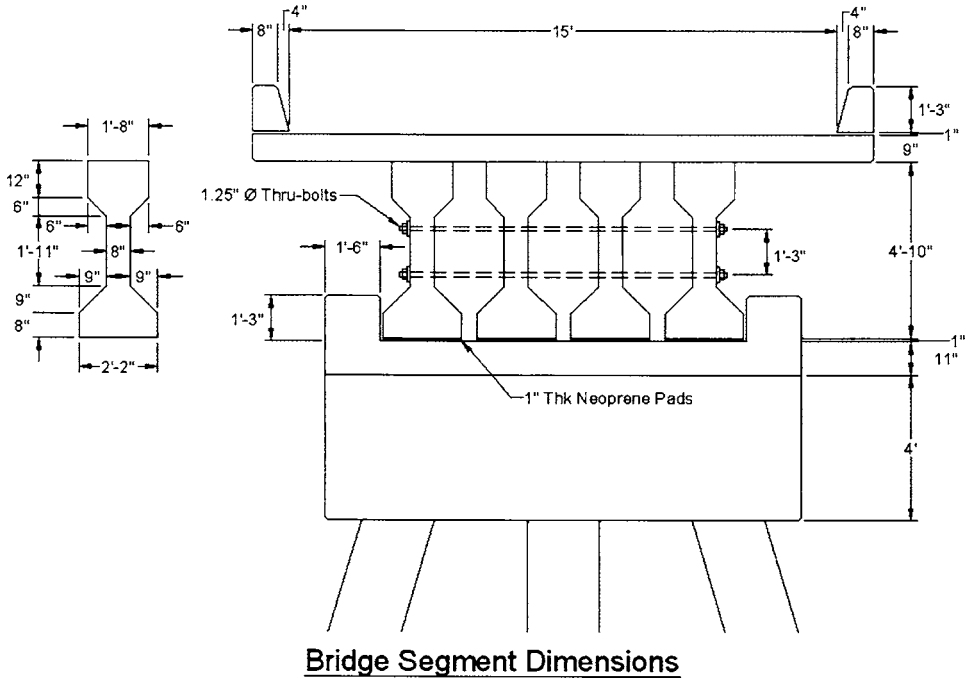

Fig. 10. Cross-section details of railroad bridge over Biloxi Bay (1 ft=0.3048 m)

webs and top slab and crushing of the concrete at the base of the webs at midspan (Fig. 11). For structures close to the shoreline, wave-induced hydrodynamic uplift and lateral loads would have added to the stress on these sections. In many cases, the negative bending failure resulted in dislocation of the double-tee ends from their supports, resulting in collapse of the floor system.

Collapse of double-tee floor systems was observed regardless of the end support details. Some double-tees were supported on continuous ledges or individual corbels, while others were supported in sockets in the spandrel beams. When supported on ledges or individual corbels, the double-tee sections are free to rise under the effects of uplift, with the only restraint provided by nominal dowel reinforcement in the topping slab. When supported in sockets in the spandrel beams, the double-tee sections are prevented from rising at these supports, but are still subject to negative bending at midspan due to the buoyancy effects of entrapped air.

Subsequent to collapse of the floor system, many of the exterior spandrel beams and interior inverted T-beams broke free from their supports because of the loss of restraint provided by the double-tees and topping slab. It is possible that some of the spandrel beam failures were caused by lateral hydrodynamic loads, but had the floor system remained intact, it would have provided lateral support for the spandrel beams, and many of the spandrel beam failures would have been prevented.

Floor System Failures

There were a number of failures of flat slab and prestressed concrete floor slab systems as a result of hydrodynamic uplift induced by surge and wave action below the second-floor level. Fig. 13 shows a multistory reinforced concrete condominium building in Biloxi with a flat slab floor system. Over half of the second-floor slab collapsed due to punching shear failure at the slab-column connections (Fig. 13). The shear failures appear to have initiated due to upward punching of the slab as a result of hydrodynamic uplift, followed by collapse under gravity load due to the absence of integrity reinforcement in the bottom of the slab passing through the supporting columns.

Each floor consists of a cast-in-place 200 mm (8 in.) thick

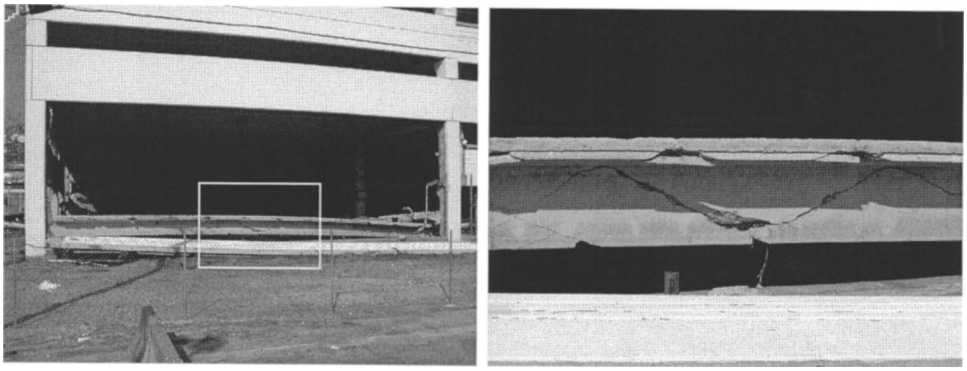

Fig. 11. Double-tee negative bending failure—parking structure in Biloxi

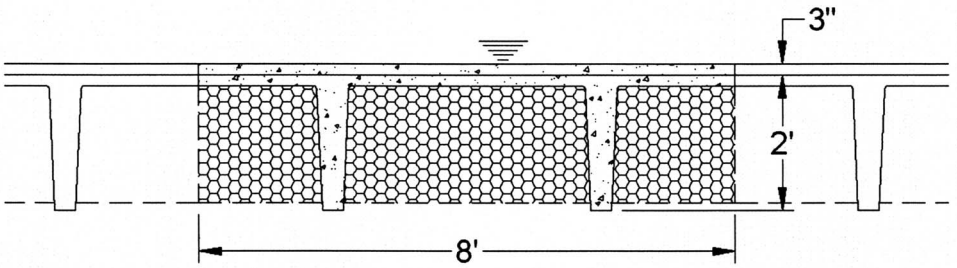

Fig. 12. Volume of air potentially trapped below a single double-tee girder (1 ft=0.3048 m)

flat plate supported on 500 by 250 mm (20 by 10 in.) rectangular columns. A typical column adjacent to the shoreline supports a tributary slab area of 20.8 m^2 (224 ft^2). Schmidt hammer testing indicated that the slab concrete strength was in the range of 28 to 35 MPa (4,000 to 5,000 psi). The ACI 318-05 (ACI 2005) design criterion for punching shear capacity under direct shear is

$$V_c = 0.33\sqrt{f'_c}b_o d = 660 \text{ kN } (150{,}000 \text{ lb}) \quad (5)$$

where f'_c=31.5 MPa (4,500 psi) (average value); $b_o=2(c_1+c_2+2d)$=2,160 mm (86 in.), the critical perimeter at $d/2$ from the column face; c_1 and c_2 are the column plan dimensions; and d=165 mm (6.5 in.), the average effective depth to the slab tension reinforcement.

Eq. (5) applies to slabs with tension reinforcement (top reinforcement) passing through the slab-column connection. For the condition of uplift, this tension reinforcement would need to be provided in the bottom of the slab. Because of the lack of bottom reinforcement passing through the slab-column connection, the punching shear capacity is estimated to be between 50 and 75% of the ACI 318-05 prediction, or 330 to 495 kN (75,000 to 112,500 lb).

A net uniform upward pressure of 15.9 to 23.8 kN/m^2 (335 to 502 psf) on the tributary area of slab is required to reach this shear capacity. Because the submerged self-weight of the concrete slab is 2.73 kN/m^2 (57 psf), the total upward pressure required to cause punching shear failure under direct shear at a slab-column connection would be 18.6 to 26.5 kN/m^2 (392 to 559 psf) on the soffit of the slab. Based on the hydrodynamic uplift estimated using Eq. (2), this would require a wave height of 1.85 to 2.64 m (6.1 to 8.7 ft) when the surge level was at the bottom of slab elevation of 2.74 m (9 ft) above grade. The maximum unbroken wave height that could occur in this water depth is approximately 2.1 m (7 ft), which is within the range required to produce punching shear failure of the slab. This analysis has assumed that the uplift does not induce bending moments at the slab-column connection, which would further reduce the punching shear capacity. In reality such bending moments would exist due to the large cantilever balcony slab protruding toward the ocean.

Collapse of the second-floor slab effectively doubled the unbraced length of the columns supporting the building above. This makes them more susceptible to failure due to buckling or debris impact. Failure of one or more columns at the base of this building could have resulted in progressive collapse of the floors above.

If these connections had been provided with integrity reinforcement in the form of continuous slab bottom reinforcement passing within the column cage, the total collapse of the floor might have been prevented, even though many of the connections would likely still have suffered punching shear failures. Integrity reinforcement is required by the ACI 318-05 building code for new concrete flat slab construction, but was not required by codes in force when this building was constructed.

An adjacent flat slab structure suffered no apparent structural damage. It was designed to support mechanical equipment for the Hard Rock Hotel and Casino and consisted of a thick flat slab with drop panels at each support column. Because of the larger design dead and live loads, this slab was presumably more heavily reinforced than the failed slab in the condominium building. It illustrates that flat slab floor systems can be designed to resist the loads applied by storm surge inundation and wave action.

Hydrodynamic uplift is also suspected of causing failure in a number of posttensioned one-way slab floor systems. A cast-in-place posttensioned parking garage at the Hard Rock Hotel

Table 4. Buoyancy Calculations for Various Normal Weight Concrete Double-Tee Sections

Double-tee designation	Width (ft)	Depth (in.)	Topping slab thickness (in.)	Air volume (ft^3/ft)	Buoyancy force (lb/ft)	Self-weight (lb/ft)	Net uplift (lb/ft)	Percent of self-weight (%)
8′−0″×24″	8	24	3	12.37	1,098	718	380	53
8′−0″×24″	8	24	2	12.40	1,057	618	439	71
8′−0″×32″	8	32	3	15.98	1,403	891	512	57
8′−0″×32″	8	32	2	16.02	1,363	791	572	72
10′−0″×24″	10	24	3	15.80	1,371	843	528	63
10′−0″×24″	10	24	2	15.84	1,320	718	602	84
10′−0″×32″	10	32	3	20.58	1,750	1,016	734	72
10′−0″×32″	10	32	2	20.63	1,700	891	809	91

Note: 1 in.=25.4 mm, 1 ft=0.3048 m, 1 lb=4.445 N.

Fig. 13. Flat slab punching shear failure due to hydrodynamic uplift

and Casino suffered significant damage and partial collapse of the second-floor bays adjacent to the coastline. It is suspected that hydrodynamic uplift loads on the slab resulted in shear failure of the slab at the supporting beams (Fig. 14) and shear failure at the ends of some of these beams (Fig. 15). The spalling of concrete cover at the epoxy-coated bottom reinforcement in the slab indicates that failure was due to uplift and not downward loads (Fig. 14).

On US 90 in Pass Christian, two multistory apartment buildings were under construction when Katrina made landfall (Fig. 16). The structural framing was complete and nonstructural finishes were being installed. The buildings were nominally identical, consisting of two levels of posttensioned (PT) concrete floors supported on cast-in-place reinforced concrete columns. The third-floor walls and roof were framed with steel and timber trusses.

Both buildings suffered partial collapse of the front section of structural concrete framing (Fig. 16). Floor slabs in the front bay (ocean side) are 178 mm (7-in.) thick PT flat slabs, spanning between 406 by 508 mm (16 by 20-in.) rectangular columns. In the second bay, 178 mm (7-in.) thick one-way slabs span between beams running perpendicular to the shore. The two-way floor slab extends 1.8 m (6 ft) in front of the front columns as cantilever balconies. The PT beams in the second bay of the building contain numerous PT tendons that extend as banded PT reinforcement into the two-way slab and cantilever balcony. Fig. 17 shows the PT anchors at the edge of the balcony slab and headed stud shear reinforcement used around the front slab-column connections supporting the flat slab section. Distributed PT tendons were also provided perpendicular to the banded PT in the two-way slab.

In one of the two buildings the front bay (closest to the shoreline) collapsed completely, while the second bay floor slab collapsed leaving the beam and column frame standing. In the second building, both front and second bays collapsed completely. The supporting columns appeared to have failed in flexure at the base and at the second-floor level, and fallen inwards away from the shoreline. As opposed to the previous flat-slab condominium slabs that failed due to negative punching shear, there is no evidence of punching shear at these slab-column connections, possibly because of the presence of headed stud shear reinforcement. This reinforcement is effective against punching in both downward- and upward-loading directions. There were no signs of debris impact and no evidence of significant debris in the area.

The failure is attributed to uplift-induced flexural failure of the one- and two-way slab systems. Failure of the one-way slab between PT beams resulted in local collapse of the slab at the second-floor level, though the integrity of the beams maintained the compression component of the PT system. Failure of the second-floor two-way slab in the front bay due to hydrodynamic uplift loading is believed to have resulted in collapse of this slab and loss of the compression component of the PT system. The numerous PT strands banded in the slab along the column lines therefore lost their compression reaction and the entire PT force would have been applied to the front columns at the second floor level. The columns would now have to span between the ground- and third-floor slab and would not have been able to resist the large lateral load applied by the PT at the second-floor level. The columns were therefore pulled inward until the tendons lost their pretension. Based on the full tendon length, the tendon elongation during stressing is estimated at 125 to 150 mm (5 to 6 in.). This would have caused flexural failure of the column at the base and

Fig. 14. Uplift-induced shear failure of a posttensioned one-way slab

Fig. 15. Shear failure of posttensioned beam supporting one-way posttensioned slab

at the level of the second-floor slab and would also have led to progressive collapse of the upper floor due to the failure of the exterior columns. In one building, the second bay beam-column frame was able to survive the collapse of the front bay, but in the second building, the interior beam-column frame collapsed, presumably as a result of the impact from the progressive collapse of the front slab-column section. This failure mechanism appears consistent with the observations made at the site and with observations of other PT slab systems that failed due to uplift loading.

Floating Structure Restraints

Overview

Significant coastal construction is often accompanied by industrial port and harbor development. In these cases, it can be anticipated that floating structures are present, in particular relatively large ships and barges. Except for near-source tsunamis, most ships should be able to evacuate the area (except those undergoing major repairs). However, it is unlikely that all barges

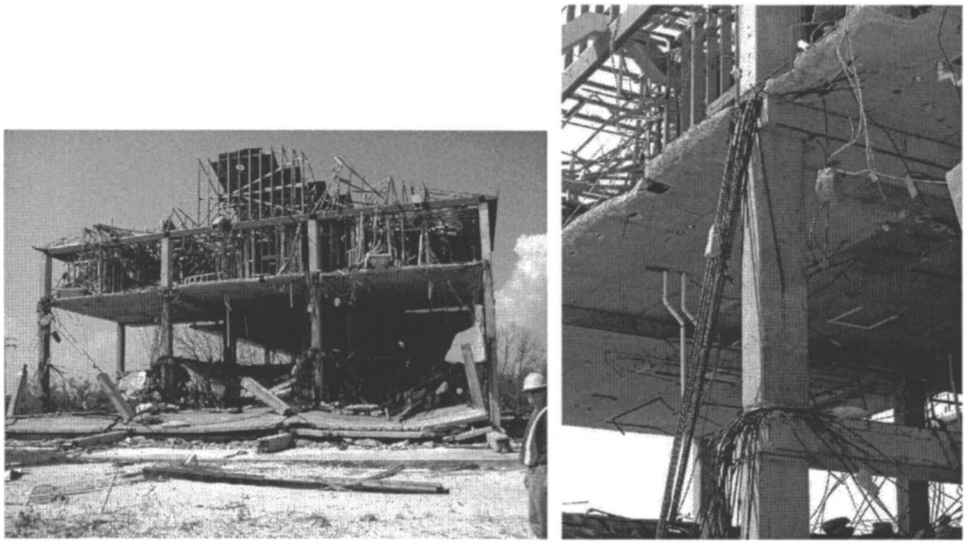

Fig. 16. Partial collapse of concrete building frame under construction

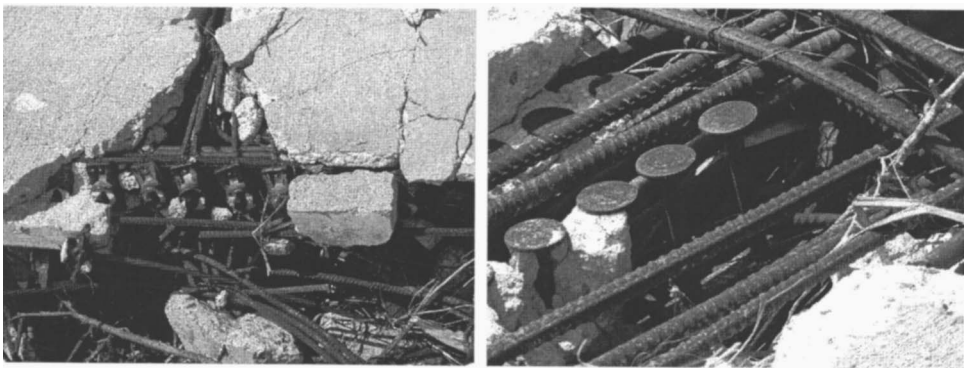

Fig. 17. Posttensioned anchors at slab edge and headed stud shear reinforcement at slab-column connection

would be able to be relocated. This was the situation in Biloxi for Hurricane Katrina, with its floating, barge-mounted casinos, and in Gulfport, which had such casinos as well as industrial barges. The mooring (restraint) systems for such structures must consider both absolute and relative motions. Several structures in Biloxi illustrate what can happen when the restraint system is not adequate.

Relative Motion between Fixed and Floating Adjacent Structures

The Hard Rock Casino was located on adjacent floating barges oriented parallel to the shore. The casino was enclosed in a fixed "shell," which was presumably designed to resist wind loads. The exterior shell collapsed onto the casino, virtually demolishing it (Fig. 18). The Hard Rock Casino was the most severely damaged of all the casinos surveyed. At least three plausible failure mechanisms can be identified. First, excessive vertical motion of the barges could have exceeded the clearance between the casino and the fixed roof, inducing collapse. The surge was estimated at approximately 6–7.5 m (20–25 ft), and this may not have been accommodated in the design. A second scenario is that the roll induced by the waves caused the top part of the casino to impact the columns of the shell, resulting in progressive collapse. The third and most likely scenario is that the surge and waves elevated and pushed the barges inland, causing the inland columns of the exterior shell to fail. With the frame resistance gone, the wind, surge, and waves then pushed the seaward columns back, and the entire system collapsed. The racking of the barges, as shown in Fig. 18, supports this hypothesis, as do other pictures that show the shore side of the first barge resting on the second floor of the shore-based structure, as well as the failure of the seaward columns.

Another example of relative motion resulting in significant collapse is the Isle of Capri casino and parking structure (Fig. 19).

Fig. 18. Hard Rock Casino barges enclosed by fixed exterior steel structure

Fig. 19. Progressive collapse of parking structure due to barge impact damage to lower-level columns

It is clear that the pounding of the barge-mounted casino on the columns of the parking structure resulted in partial progressive collapse. It is unlikely that the light-frame superstructure could have caused the collapse of the concrete columns. It is more likely that the barge hull, which was located very close to the exterior columns, slammed into the columns as a result of increase in elevation, roll, and/or yaw. The floor system, consisting of posttensioned one-way slabs supported on long-span, posttensioned beams, was unable to prevent progressive collapse without the column support. The relative positioning of the collapsed

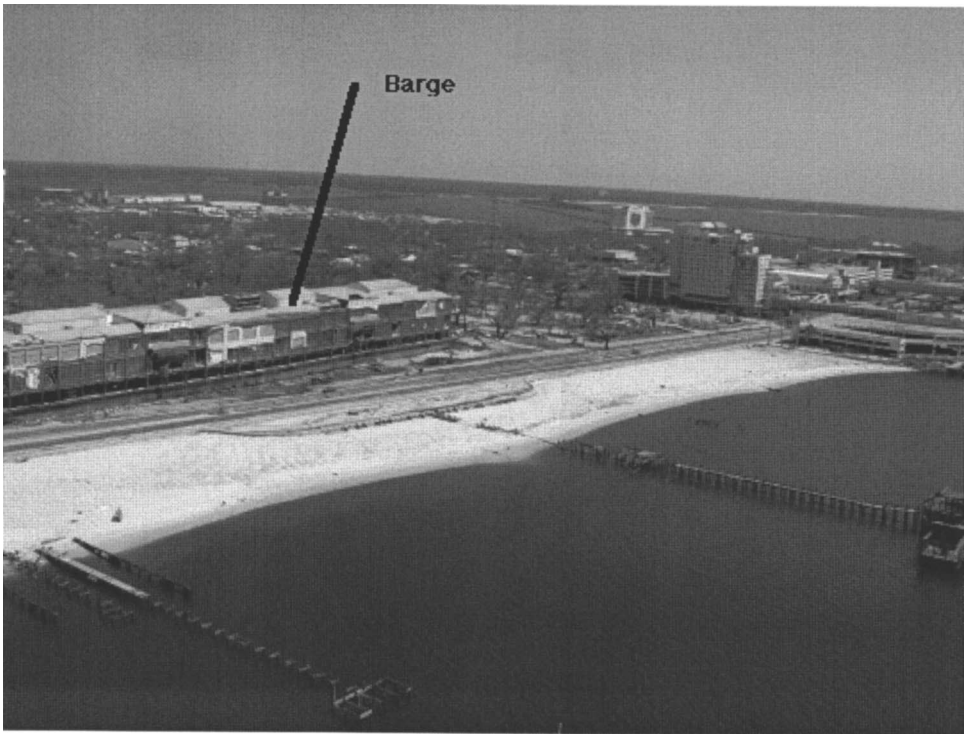

Fig. 20. Larger Grand Casino Biloxi barge transported alongshore and inland by Hurricane Katrina (Photo courtesy of U.S. National Oceanic and Atmospheric Administration/Department of Commerce)

Fig. 21. Damage to cast-in-place reinforced concrete building caused by impact of adjacent barge

spandrel beams indicates that the middle floors likely collapsed first. The long span of the slab could not be supported without the column, causing the upper floors to collapse and then finally the lower floors. Note the mooring piles, which were inadequate to prevent the destructive impact.

There are several design decisions that could have prevented this collapse. Clearly a better-designed mooring system could have prevented the barge from impacting the building. In addition, if the exterior columns had been inset away from the edge, they would then have been protected by the floor slabs, which would have acted as giant bumpers. The garage structure could also have been designed to resist progressive collapse so that damage to a few columns would not result in disproportionate collapse of the floor slabs.

Restraint against Lateral Movement

The Grand Casino Biloxi consisted of two barge-mounted, multistory casino structures. These broke free from the dolphin mooring system and were transported a substantial distance onshore (Fig. 20). The smaller, three-story casino barge was approximately 39 m (100 ft) wide, and 60 m (200 ft) long and had a draft

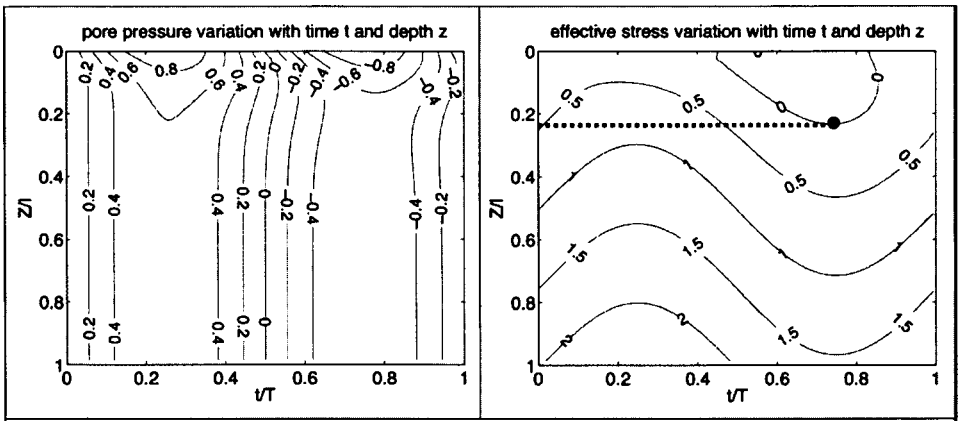

Fig. 22. Predicted pore pressure and effective stress variation based on 1D calculation (1 ft=0.3048 m)

Fig. 23. Liquefaction-induced scour under fill-supported first-floor slab

of approximately 2.4 m (8 ft). The single-family house next to its resting place was demolished, and the casino caused severe damage to the abandoned Tivoli Hotel when it collided (Fig. 21). There appeared to be minimal damage to the barge hull. This failure will be discussed subsequently.

Effects of Scour

Types of Scour

Extensive scour was observed around bridge abutments and piers, building foundations, and highway pavement structures along the affected areas of the Gulf Coast. This scour contributed to the partial or complete collapse of a number of coastal structures. Two types of scour mechanism were identified: (1) shear-induced scour due to pickup and transport of sediments by the flowing water and debris; and (2) liquefaction-induced scour due to soil instability as a result of pore pressure gradients within the sediment bed. Although both mechanisms contributed to the scour of beaches and coastal structures, liquefaction-induced scour is believed to be responsible for the extensive scour damage observed under building foundations and highway pavements.

During a storm surge event, liquefaction-induced scour occurs when the vertical effective stress between soil particles is reduced to nearly zero due to phase difference (i.e., time lag) between pore-pressure variation in the soil and water pressure variation on the bed surface. This mechanism is enhanced by the rapid drawdown as the surge water recedes. Scour can occur very rapidly under such conditions because the soil loses almost all of its shear strength and thus behaves like a viscous liquid, which can be transported easily by the flowing fluid.

During Hurricane Katrina, the storm surge lasted for several hours and exceeded 7.5 m (25 ft) along portions of the Mississippi coastline. The nearly saturated sandy deposits also were subjected to pressure fluctuations due to wave actions, which can also result in liquefaction-induced scour. As demonstrated in Fig. 22, at a water depth of 4.5 m (15 ft) and a wave height of 3 m (10 ft), the depth of liquefaction of nearly saturated sand deposits can reach up to 0.75 m (2.5 ft) below the seabed surface. This wave-induced liquefaction can be even more severe during wave drawdown or ebb surge due to rapid decrease of the water level, without time for the internal pore pressure to dissipate.

Wave-induced liquefaction is also believed to be responsible for the scour under ground-floor slabs and highway subgrades (Figs. 23 and 24). The thin floor slab or highway pavement helps to prevent shear-induced scour and postpone the point at which liquefaction occurs. Nevertheless, the supporting sandy soil or backfill is still susceptible to liquefaction-induced scour, particularly during wave drawdown or ebb surge. Once the supporting soil liquefies and is carried away by the flowing fluid, the thin floor slab or highway pavement, which initially rested on the soil, will collapse, which may eventually lead to total collapse of the structure. Numerous examples of liquefaction-induced scour under floor slabs and footings were observed throughout the Mississippi coastline. Sinkhole-like craters also were observed in many locations along the coastal highways due to drawdown and wave-induced liquefaction of the subgrade below the pavement (Fig. 24).

The most extensive scour observed along the Mississippi coastline was at the west-end abutment of the US 90 bridge in the town of Bay St. Louis (Fig. 25). The abutment was originally surrounded by a soil embankment protected by a retaining wall and concrete apron. Massive scour of all backfill and sand subsoil was observed below the collapsed reinforced concrete embankment apron, which led to the exposure of the piled foundation below. The maximum scour depth was approximately 4.5 m (15 ft), and the scour extended behind the abutment wall and undermined the approach slabs by as much as 2.5 m (8 ft). A combination of wave-induced liquefaction and shear-induced scour is also believed to be responsible for the complete failure of Beach Boulevard in Bay St. Louis, where the maximum scour depth was around 1.5–1.8 m (5–6 ft) (Fig. 26). A number of residential and low-rise commercial buildings also suffered foundation failure and partial building collapse due to undermining by scour (Fig. 27).

Effects of Debris

Types of Debris

Katrina demonstrated that any floating or mobile object in the nearshore/onshore areas can become floating debris. This includes shipping containers, boats, unrestrained storage containers, eighteen wheeler trucks, and barges. As the debris accumulates, floating debris fields can develop that can cause substantial loads as they block the fluid flow. Debris effects on structures took two forms: impact and water damming.

Impact

An example of impact is clearly demonstrated by the collision of the Grand Casino barge with the Tivoli Hotel (Fig. 21). The 2.4 m

Fig. 24. Sinkhole-like crater left by scour of liquefied subgrade below coastal highway

(8 ft) draft of the barge, as reported above, was estimated from the water line on the barge hull. If this was indeed the draft during the storm, then the barge's mass was approximately 4,600 t. Such a mass, with only a modest speed, will impose a large force on any structure it impacts. ASCE/SEI 7-05 (ASCE 2005) suggests the following formula for impact forces:

$$F = \frac{\pi WV}{2g\Delta t} \tag{6}$$

in which W=weight, V=impact velocity, g=gravity, and Δt= impact duration (the additional coefficients in the code equation are taken to be 1.0). This equation is based on simple

Fig. 25. Up to 4.5 m (15 ft) of scour around abutment exposing piles below abutment

Fig. 26. Complete scour of Beach Boulevard in Bay St. Louis

impulse-momentum considerations and assumes the time variation of the impact force is a quarter-cosine wave. ASCE 7 recommends 0.03 s as the impact duration, while the *Coastal Construction Manual* (CCM) (FEMA 2000) recommends approximately 0.3 s (with a slightly different formula). If we assume the 4,600 t barge had a modest 2.24 m/s (5 mph) impact velocity and a 0.03 s impact duration, the maximum impulsive force acting on the structure is approximately 540 MN (120,000 kips). Even one-tenth of such a lateral load is well above the capacity of any practical column. Hence, in such environments it

Fig. 27. Scour under foundations leading to partial collapse of residence

Fig. 28. Empty steel shipping container lodged against columns supporting roof

is critical to ensure that progressive collapse does not result when a small number of columns or walls are damaged.

Although the impact demolished a corner column in the reinforced concrete building, the fifth floor and roof remain intact; this demonstrates the intrinsic redundancy in reinforced concrete buildings even when not specifically designed to prevent progressive collapse. In more usual cases, the mass will be substantially less but the velocities will likely be much higher, especially in the case of a tsunami. However, except for slender steel tubular columns, no significant structural damage was observed as a result of impact except in the case of the barge casinos. The design engineer can obtain some guidance from ASCE 7 and CCM, but, current code provisions do not appear to provide adequate protection against collapse as a result of impact from "large" debris. Recent work may help to improve some code specifications relating to impact forces (Trimbath 2006).

Water Damming

In addition to impact damage, there was clear evidence of damage from the water-damming effect. This happens when "large" debris becomes lodged against structures, perhaps broadside, and there are significant drag and inertia forces that result from the disruption in the flow field.

Shipping containers are ubiquitous and therefore represent a common type of debris that can cause substantial fluid forces on structures, even those that under normal circumstances would be considered relatively wave transparent. Fig. 28 illustrates this situation, where a shipping container bridged between two slender steel pipe columns supporting the roof of a car dealership. As evidenced by the crumpling of the upstream side of the 6 m (20 ft) standard container, significant hydrodynamic forces resulted from this "damming" effect. The steel columns held, but not without significant damage. The 127 mm (5 in.) diameter columns were 4.57 m (15 ft) on center and 6.0 m (20 ft) high, the pipe wall thickness was likely either 6.35 or 9.5 mm (1/4 in or 3/8 in.), and the yield stress is likely 290 MPa (42 ksi) (these are typical values). For simplicity, we assume the columns are simply supported and the top of the container resulted in a force at the column midspan. The concentrated midspan force that would develop full yielding of the column cross section based solely on

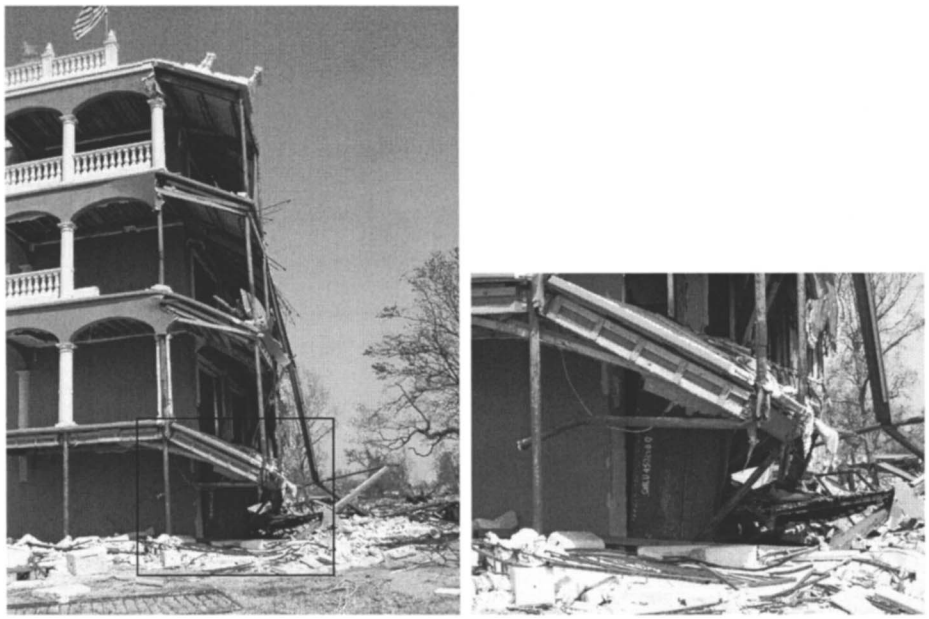

Fig. 29. Shipping container damage to steel pipe columns supporting balconies

Fig. 30. Bending failure of piles due to shipping container impact and damming effect

bending would be 16.5 or 23.6 kN (3.7 or 5.3 k), respectively, for the two likely wall thicknesses. The drag force can be estimated from

$$F_D = C_D \frac{\rho V^2}{2} A \tag{7}$$

in which C_D=drag coefficient, ρ=fluid density, V=fluid velocity, and A=projected area. The commentary to ASCE 7-05 (ASCE 2005) mentions a drag coefficient of 1.0, which would seem to be a minimum value. As a simplification, it is assumed here that the total drag force was distributed such that one-fourth was applied to a single column midspan. Under these assumptions, the fluid velocity required to obtain the failure forces is only approximately 2.9 to 3.4 m/s (6.5 to 7.5 mph), a moderate velocity. As a result, it can be seen that the damming effect can significantly increase the forces on slender structural members and easily lead to failure. Fig. 29 shows the damage a shipping container caused to an apartment building. This damage likely resulted from a combination of debris impact and damming. In any event, the failure of the steel pipe columns at the first level resulted in progressive collapse of the upper level balconies.

Fig. 30 shows the failure of numerous piles that had been installed in anticipation of expanding the adjacent industrial facility. The shipping container was pushed along by the water and leveled rows of concrete piles. Although the first few piles may have failed as a result of impact, it is likely that the later piles (and possibly all of them) failed as a result of the damming effect caused by the container being broadside to the fluid flow.

The 300 mm (12 in.) square piles were prestressed with four 13 mm (0.5 in.) diameter tendons located at each corner of the cross section. Based on the measured location of these tendons, an assumed concrete compressive strength of 41 MPa (6,000 psi), and an assumed tendon ultimate tensile strength of 1,860 MPa (270 ksi), the bending capacity of each pile is estimated at 76.5 kN·m (56.4 ft-kip). Pile failure occurred at approximately 0.6 m (2 ft) below grade, while 2.4 m (8 ft) of pile was exposed above grade. Assuming a standard 12.2 m (40 ft) container lodged against three of the piles, spaced at 3.7 m (12 ft) on center, an average lateral pressure of 3.7 kN/m (78 psf) on the container would cause pile failure. Using the same assumptions presented earlier for estimating the drag force on the shipping container, this pressure would be developed by a moderate fluid velocity of 2.7 m/s (6.1 mph). Although these piles were particularly susceptible to bending failure as freestanding cantilevers, these failures demonstrate the considerable potential for damage due to debris-damming effects.

Summary

Hurricane Katrina resulted in very large storm surge along the Gulf Coast, especially in Mississippi. The hardest-hit areas, from Biloxi to Pass Christian, suffered a storm surge of approximately 6–7.5 m (20–25 ft), which resulted in substantial damage to some engineered structures. In the case of low-lying bridges, segments were lifted up by a combination of hydrostatic (from submersion) and hydrodynamic (from waves) forces and then displaced laterally by the hydrodynamic forces from surge and waves. Similarly, parking garage floor systems constructed of precast double-tee beams, which are weak in negative bending, suffered numerous collapses as a result of these uplift forces. Condominiums and other building structures also suffered substantially if the slab systems were not able to handle the unanticipated uplift forces.

Katrina demonstrated that any floating/mobile object can become floating debris. In this case, the debris included floating casino barges, industrial barges, shipping containers, and 18-wheeler trucks. Several damage modes can be identified. Fixed structures adjacent to floating structures were damaged by the large relative motion. For casino barges that broke free, while the velocities were likely relatively small, their large mass meant that the momentum was still substantial when impact occurred, causing large impulsive forces. Smaller debris also poses risks to structures, including those resulting in flow damming. Even wave-transparent structures, such as those on columns, can be subjected to large forces when, for example, shipping containers become lodged against the columns, damming the water and increasing by multiple times the surface area exposed to the flow.

Substantial scour resulted from both shear-induced sediment transport and liquefaction induced flow resulting from rapid pore-pressure changes in sandy backfill and subsurface deposits. Scour due to liquefaction occurred in backfill below foundation slabs and highway pavements, even though these soils were protected from shear-induced scour by the overlying structure.

This survey demonstrated that engineered structures in regions subject to hurricane-induced storm surge or tsunami inundation have significant risk factors associated with sometimes unanticipated loads, such as uplift, debris impact and damming, and liquefaction-induced scour. Engineers, developers, insurers, and building officials should be aware of these unusual loading conditions to achieve better risk assessment for and management of coastal facilities.

Conclusions and Recommendations

Based on analysis of the observations made during reconnaissance surveys of the coast affected by the storm surge from Hurricane Katrina, the following conclusions were drawn.

- Many engineered structures in the Katrina inundation zone experienced only nonstructural damage at the lower levels due to the storm surge and storm wave action. A number of structures experienced significant structural damage due to the effects of the coastal inundation.
- Bridge decks and structural floor systems submerged during coastal inundation are subjected to significant hydraulic loads, including hydrostatic uplift due to buoyancy, which is amplified by the effect of entrapped air, and hydrodynamic uplift due to vertical wave action. These loads are dynamic and highly variable and were probably repeated a number of times during an inundation event. If structural design is performed using equivalent static forces, the dynamic nature of the actual loading condition must be considered so as to incorporate adequate ductility and toughness in the members and their connections.
- Deck segments of low-level bridges in regions subject to coastal inundation should be restrained against uplift and provided with shear keys designed to resist all anticipated lateral loads, ignoring the contribution of gravity-induced friction. Bulkheads and blocking should be designed to allow air to escape from below the deck, thereby reducing the volume of trapped air when submerged.
- Building floor systems below the anticipated inundation level should be designed for uplift due to buoyancy, including the effect of entrapped air, and hydrodynamic uplift due to wave action. Prestressed double-tee systems are particularly susceptible to uplift failure due to the large volume of entrapped air between the tee webs and the uplift induced by the prestress design. Flat slab and other concrete floor systems must also be designed for hydrodynamic uplift forces produced by wave and surge action. These forces induce inverted bending and shear effects on continuous floor systems typically designed only for gravity loads.
- Restraint systems for floating structures such as barges should be designed to permit water elevation changes anticipated during the design event. The restraint systems should also be designed for the lateral loads induced by the surge and wave action.
- The primary effects of floating debris are the initial impact when debris strikes a structural element and the damming effect if the debris lodges against the structural element. The types of debris will vary with the coastal location. Standard shipping containers should be considered as the design debris in many developed coastal areas.
- Multistory buildings should be designed for progressive collapse prevention in the event of unforeseen damage to individual structural elements at the lower levels.
- Building and bridge foundations must be designed to accommodate scour induced by the surge and wave action. Scour results from both shear-induced particulate transport and liquefaction-induced soil flow.
- Backfill around foundations and under earth-supported slabs should be selected to avoid liquefaction during rapid drawdown. Soil stabilization could be considered to reduce or prevent both liquefaction and shear-induced scour.

Acknowledgments

Two reconnaissance trips were made by the writers to the Mississippi coastline at the end of September and early November 2005. The writers wish to thank Brian Drake and his colleagues at Keesler Air Force Base for their assistance with on-base accommodations during both trips. Funding was provided by the National Science Foundation (NSF) under a Small Grant for Exploratory Research (Grant No. #0553966) and through the NSF George E. Brown, Jr. Network for Earthquake Engineering Simulation (Grant No. #0530759). This funding is gratefully acknowledged.

References

ACI 318-05. (2005). *Building code requirements for structural concrete and commentary*, American Concrete Institute, Farmington Hills, Mich.

ASCE. (2005). *Minimum design loads for buildings and other structures*, *ASCE/ESI 7-05*, ASCE, Reston, Va.

Bea, R. G., Xu, T., Stear, J., and Ramos, R. (1999). "Wave forces on decks of offshore platforms." *J. Waterway, Port, Coastal, Ocean Eng.*, 125(3), 136–144.

Canadian Association for Earthquake Engineering (CAEE). (2005). *Reconnaissance Rep. on the December 26, 2004 Sumatra Earthquake and Tsunami*, June.

Chen, Q., Zhao, H., Hu, K., and Douglass, S. L. (2005). "Prediction of wind waves in a shallow estuary." *J. Waterway, Port, Coastal, Ocean Eng.*, 131(4), 137–148.

Dengler, L. A., and Magoon, O. T. (2005). "The 1964 tsunami in Crescent City, California: A 40-year retrospective." *Solutions to coastal disasters 2005*, ASCE, Reston, Va., 639–648.

Douglass, S. L., Chen, Q., Olsen, J. M., Edge, B. L., and Brown, D. (2006). "Wave forces on bridge decks." *Draft Rep. for Federal Highway Administration*, Office of Bridge Technology, Washington, D.C.

Federal Emergency Management Administration (FEMA). (2000). *Coastal construction manual*, FEMA 55, Washington, D.C.

Federal Emergency Management Administration (FEMA). (2006a). *Hurricane Katrina in the Gulf Coast Summary Rep.*, FEMA 548, March.

Federal Emergency Management Administration (FEMA). (2006b). *Hurricane Katrina in the Gulf Coast: Observations, recommendations, and technical guidance*, FEMA 549, March.

Louisana State Univ. (LSU). (2005). LSU Hurricane Center, ⟨http://hurricane.lsu.edu/⟩ (Sept. 2005).

Mosqueda, G., and Porter, K. P. (2006). "Preliminary conclusions—Assessing damage to engineered buildings in the wake of Hurricane Katrina." *Struct. Eng.*, 7(2), 20–26.

Rogers, S. M., Jr. (2005). "Coastal building performance in Hurricane Isabel: Backward trends in design." *Solutions to coastal disasters 2005*, ASCE, Reston, Va., 514–523.

Saatcioglu, M., Ghobarah, A., and Nistor, I. (2005). *Reconnaissance Rep. on the December 26, 2004 Sumatra Earthquake and Tsunami*, Canadian Association for Earthquake Engineering, June.

Tezak, E. S., and Rogers, S. (2005). "FEMA sponsored coastal structures damage assessment in North Carolina for Hurricane Isabel (HMTAP task order 274, Sept. 2003)." *Solutions to coastal disasters 2005*, ASCE, Reston, Va., 524–537.

Trimbath, K. (2006). "Barge impact study could lead to better bridge specifications." *Civ. Eng. (N.Y.)*, 76(1), 29–30.